Computation of Torques in Magnetic Tunnel Junctions through Spin and Charge Transport Modeling

Simone Fiorentini
Christian Doppler Laboratory for NovoMemLog at the Institute for Microelectronics TU Wien
Vienna, Austria
fiorentini@iue.tuwien.ac.at

Johannes Ender
Christian Doppler Laboratory for NovoMemLog at the Institute for Microelectronics TU Wien
Vienna, Austria
ender@iue.tuwien.ac.at

Mohamed Mohamedou
Christian Doppler Laboratory for NovoMemLog at the Institute for Microelectronics TU Wien
Vienna, Austria
mohamedou@iue.tuwien.ac.at

Roberto Orio
Institute for Microelectronics TU Wien
Vienna, Austria
orio@iue.tuwien.ac.at

Siegfried Selberherr
Institute for Microelectronics TU Wien
Vienna, Austria
selberherr@iue.tuwien.ac.at

Wolfgang Goes
Silvaco Europe Ltd
Cambridge, United Kingdom
wolfgang.goes@silvaco.com

Viktor Sverdlov
Christian Doppler Laboratory for NovoMemLog at the Institute for Microelectronics TU Wien
Vienna, Austria
sverdlov@iue.tuwien.ac.at

***Abstract*—Spin-transfer torque based devices are among the most promising candidates for emerging nonvolatile memory. Reliable simulation tools can help understand and improve the design of such devices. In this paper, we extend the drift-diffusion approach for coupled spin and charge transport, commonly applied to determine the torque in metallic valves, to the case of magnetic tunnel junctions, which constitute the cell of modern spin-transfer torque memories. We demonstrate that, by introducing a magnetization dependent conductivity and properly choosing the spin diffusion coefficient in the tunnel barrier, the expected behavior of both, the electric current and the spin accumulation, is properly reproduced. The spin torque values' dependence on the system parameters is investigated. As a unique set of equations is used for the entire memory cell, this constitutes the basis of an efficient finite element based approach to rigorously describe the magnetization dynamics in emerging spin-transfer torque memories.**

Keywords—Spin and charge drift-diffusion, spin-transfer torque, magnetic tunnel junctions, STT-MRAM

I. Introduction

Nonvolatility is an emerging solution to the high stand-by power leakages due to the downscaling of the dimensions of traditional semiconductor components. Spin-transfer torque magnetoresistive random access memory (STT-MRAM) is a viable nonvolatile component, thanks to its simple structure and compatibility with CMOS technology. It possesses both high speed and excellent endurance, as well as low fabrication costs, and is thus promising for applications ranging from IoT and automotive uses to embedded DRAM, and last level caches [1]- [7].

The binary information in modern magnetic memories is stored as the relative orientation of the magnetization in the free and reference layers of a magnetic tunnel junction (MTJ) schematized in Fig.1. The magnetization in the free layer can be switched by a current through the structure. The electrons get spin polarized by the reference layer and, when entering the free layer, transfer their polarization to the magnetization, providing the torque.

Accurate simulations of the magnetization dynamics in these structures provide a way of improving the design of future devices. Our aim is to demonstrate a finite element method (FEM) simulation tool for efficiently predicting the behavior of spintronic devices. The focus of this work is to extend the drift-diffusion approach for the computation of the torques to the case of a magnetic tunnel junction.

II. Magnetization Dynamics

Accurate simulation tools are a powerful support in the design of STT-MRAM devices. The description of the magnetization **m**, subject to the spin-transfer torque, is given by the Landau-Lifshitz-Gilbert equation

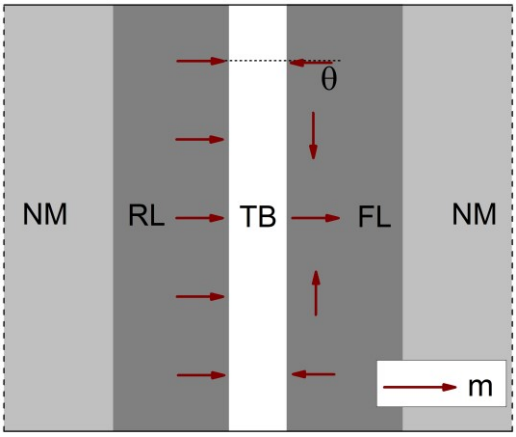

Figure 1. MTJ structure with magnetization in the free layer going from parallel in the center to antiparallel on the sides. The structure is composed of reference layer (RL), tunnel barrier (TB), free layer (FL) and two non-magnetic contacts (NM).

$$\frac{\partial \mathbf{m}}{\partial t} = -\gamma\mu_0 \mathbf{m}\times\mathbf{H}_{\text{eff}} + \alpha\mathbf{m}\times\frac{\partial \mathbf{m}}{\partial t} + \frac{1}{M_S}\mathbf{T}_\mathbf{S}, \quad (1)$$

where $\mathbf{m}=\mathbf{M}/M_S$ is the position-dependent normalized magnetization, M_S is the saturation magnetization, α is the Gilbert damping constant, γ is the gyromagnetic ratio, μ_0 is the vacuum permeability, and $\mathbf{H}_{\text{eff}}$ is the effective magnetic field, containing various contributions such as the external field, the exchange interaction, the anisotropy field, and the demagnetizing field.

Modeling of STT switching can be performed by assuming Slonczewski-like torque expressions [8]. This, however, allows to approximately simulate the magnetization dynamics of the free layer only. A more complete description of the process can be obtained by computing the non-equilibrium spin accumulation $\mathbf{S}$ across the whole structure. In this case, the torque takes the form [9], [10]

$$\mathbf{T}_\mathbf{S} = -\frac{D_e}{\lambda_J^2}\mathbf{m}\times\mathbf{S} - \frac{D_e}{\lambda_\varphi^2}\mathbf{m}\times(\mathbf{m}\times\mathbf{S}). \quad (2)$$

The torque $\mathbf{T}_\mathbf{S}$ is created by the spin accumulation acting on the magnetization. λ_J is the exchange length, λ_φ is the spin dephasing length, and D_e is the electron diffusion coefficient in the ferromagnetic layers. The spin accumulation is generated, when an electric current passes through the structure, thanks to the polarizing effect of the background magnetization. In order to compute $\mathbf{S}$, coupled spin and charge transport must be resolved. This requires taking into account that the cells in STT-MRAM devices consist of *magnetic tunnel junctions* (MTJ), a sandwich of two ferromagnets separated by a *tunnel barrier*. The tunnel barrier is essential to achieve a high tunneling magnetoresistance ratio (TMR), related to the large difference in the conductances G_P and G_{AP} in the parallel/anti-parallel MTJ configuration.

$$\text{TMR} = \frac{G_P - G_{AP}}{G_{AP}} \quad (3)$$

III. Current Density Computation

The resistance of the tunnel barrier defines the current through the MTJ, as it is much larger than the resistances of the conductive layers. To compute the current through the structure, we model the tunnel barrier as a poor conductor whose low conductivity depends on the ***relative orientation of the magnetization*** in the ferromagnetic layers as

$$\sigma(\theta) = \sigma_0\left(1+\left(\frac{\text{TMR}}{2+\text{TMR}}\right)\cos(\theta)\right), \quad (4)$$

where σ_0 is the average between the conductivities in the P and AP state, and θ is the local angle between magnetic vectors in the free and reference layers. To obtain the current, we solve

$$\nabla\cdot(\sigma\nabla V) = 0, \quad (5a)$$

$$\mathbf{J_C} = \sigma\nabla V, \quad (5b)$$

where σ is the conductivity, V is the electrical potential, and $\mathbf{J_C}$ is the current density. The equation is solved with the magnetization configuration schematized in Fig.1. The potential is fixed by Dirichlet conditions on the left and right boundaries, which are defined by the applied voltage. The conductivity is constant in the ferromagnetic layers and in the

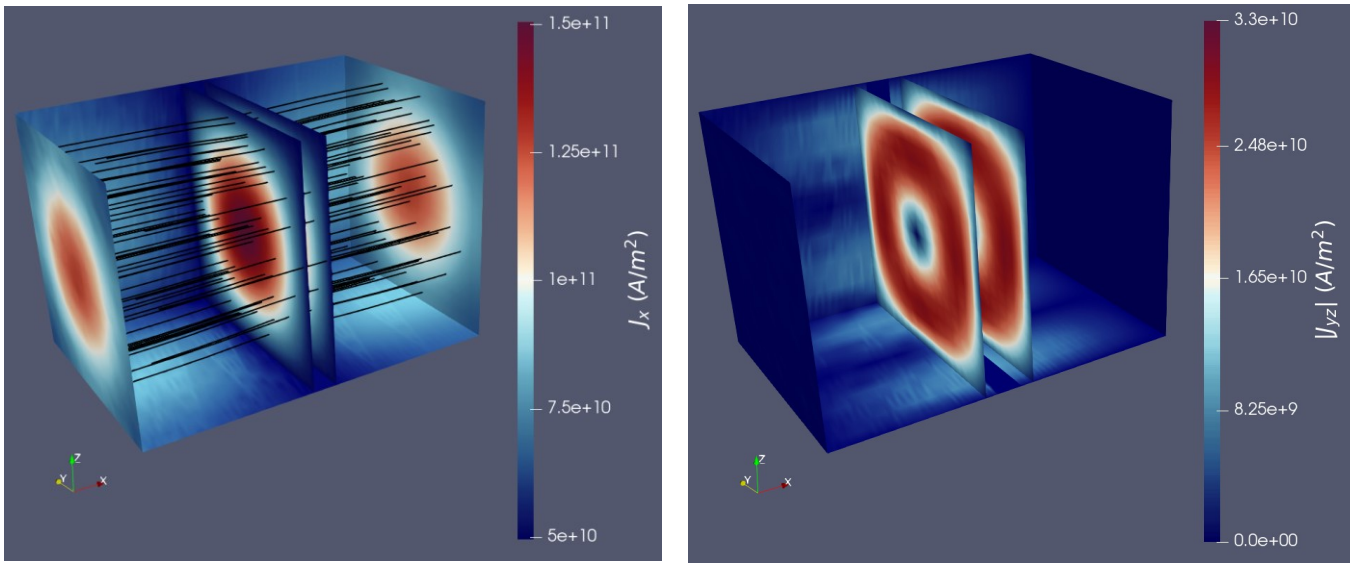

Figure 2. Current density distribution through a square MTJ with a non-uniform magnetization. The left panel shows the x-component (perpendicular) of the current density, while the right panel shows the modulus of the y- and z- (in-plane) components. The x-component flow is higher for aligned magnetizations because of the lower resistance. Due to conservation of the current flow, it is redistributed in the yz-plane in the metal contacts (right panel).

TABLE I: DRIFT-DIFFUSION PARAMETERS OF THE MAGNETIC REGIONS

Parameter	*Value*
Current spin polarization, β_σ	0.9
Diffusion spin polarization, β_D	0.8
Electron diffusion coefficient, D_e	$2\text{x}10^{-3}$ m^2/s
Spin-flip length, λ_{sf}	10 nm
Exchange length, λ_J	2 nm
Spin dephasing length, λ_φ	5 nm

non-magnetic leads, while it is described by (4) in the tunneling layer. The solution for the current in this scenario is computed via the finite element method and is reported in Fig.2 for a TMR of 200%. This TMR value is comparable to those reached in typical present devices [11]. The computed current is highly non-uniform and is redistributed to accommodate the varying conductivity in the middle layer. In particular, the x-component of the current is highest in the center of the structure, where the magnetization vectors are parallel, and lowest on the sides, where the vectors are antiparallel. The in-plane components try to make the current converge towards the center. This shows that, for non-uniform relative magnetization, characteristic to switching, the conductivity and current in an MTJ depend strongly on the position. By the described method, we can obtain the current at every time step, and use it to compute the spin accumulation.

IV. SPIN ACCUMULATION COMPUTATION

Obtaining a good approximation of the current density $\mathbf{J}_C$ is not sufficient to model spin transport in MTJs. Once the current $\mathbf{J}_C$ is known, the spin accumulation and the spin current density $\mathbf{J}_S$ are found as [10], [12]

$$\mathbf{J_S} = \frac{\mu_B}{e}\beta_\sigma\left(\mathbf{J_C}+\beta_D D_e \frac{e}{\mu_B}[(\nabla \mathbf{S})\mathbf{m}]\right)\otimes\mathbf{m}\text{-}D_e\nabla\mathbf{S}, \quad (6a)$$

$$\text{-}\nabla\mathbf{J_S}\text{-}D_e\left(\frac{\mathbf{S}}{\lambda_{sf}^2}+\frac{\mathbf{S}\times\mathbf{m}}{\lambda_J^2}+\frac{\mathbf{m}\times(\mathbf{S}\times\mathbf{m})}{\lambda_\varphi^2}\right)=0, \quad (6b)$$

where μ_B is the Bohr magneton, e is the electron charge, β_σ and β_D are polarization parameters, λ_{sf} is the spin-flip length, and $\otimes$ stands for the tensor product.

One must also ensure that the spin accumulation is preserved across the barrier, as in the case of ideal tunneling with no spin-flips. Equations (6a) and (6b) in the middle layer reduce to

$$D_S\nabla^2\mathbf{S} - D_S\frac{\mathbf{S}}{\lambda_{sf}^2} = 0, \quad (7)$$

where we indicate with D_S the diffusion coefficient in the middle layer. The first step to prevent **S** from decaying in the middle layer is to assume the spin flip length is infinite in the tunnel layer. However, this is not sufficient. The ***spin diffusion coefficient*** in the barrier region, which is a parameter one is free to choose, must also be taken considerably ***larger*** compared to the electron diffusion coefficient in the ferromagnetic layers, as shown in Fig.3. If the two coefficients have the same value, the spin accumulation decays linearly through the tunnel barrier, while the choice of a large spin diffusion coefficient reduces the slope in the middle layer to the point that the spin accumulation is practically preserved. The parameters of the magnetic regions used in the simulations are reported in Table 1.

With **S** known, we can compute the torques acting on the magnetization. Fig.4 shows the dependence between the torque acting on the free layer and the choice of the spin diffusion coefficient. Provided that the value of the latter is

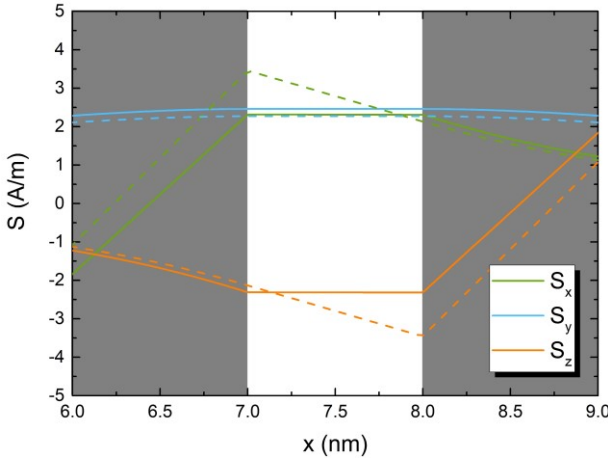

Figure 3. Spin accumulation across the middle layer, with magnetization along z in the FL and along x in the RL. The dashed lines use the same value for D_S in TB and D_e in the FL/RL, while solid lines use a very high value of D_S.

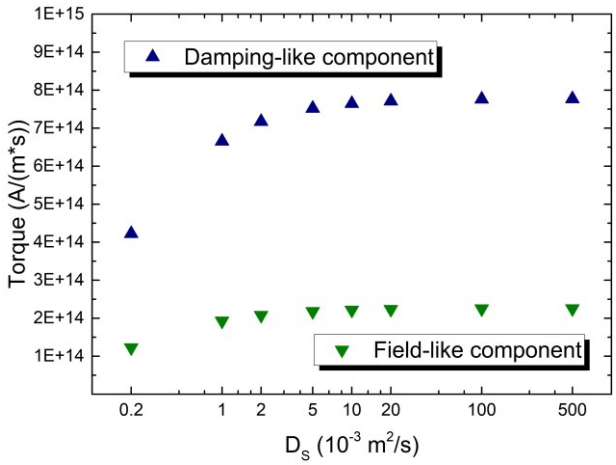

Figure 4. Magnitude of the torque in the FL as a function of the spin diffusion coefficient in the TB. At high values of the coefficient, the torque does not depend on it.

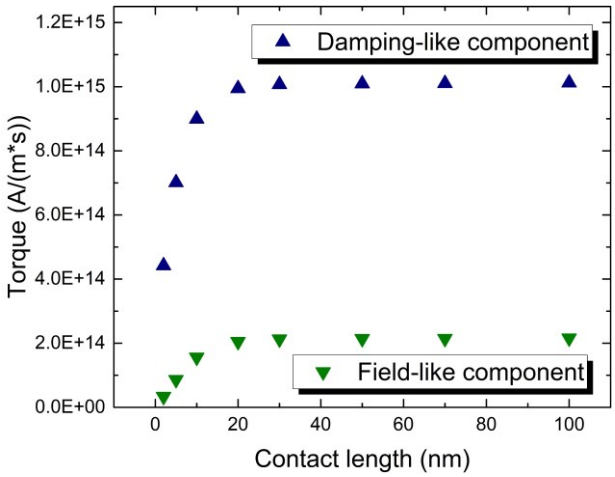

Figure 5. Magnitude of the torque in the FL as a function of the non-magnetic contact length. For a length of 30 nm or more, the torque becomes independent of it.

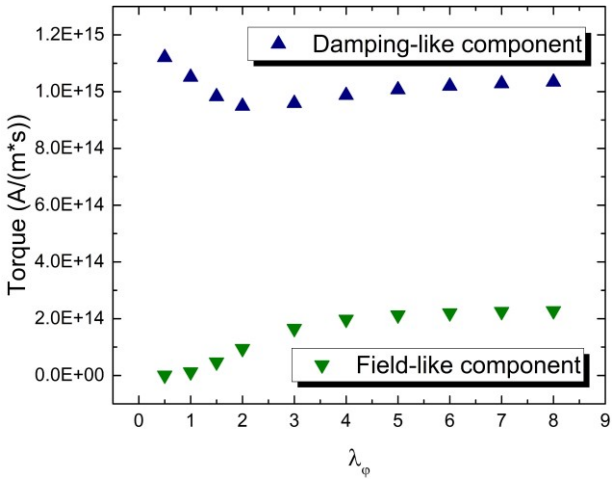

Figure 6. Magnitude of the torque in the FL as a function of the spin dephasing length. For values lower than 3 nm, the contribution of λ_φ to the total torque becomes substantial.

chosen large enough, the torque does not depend on it. In Fig.5 we report the dependence of the torque on the length of the non-magnetic contacts. The results show that a contact length of at least 30 nm is required to let the spin accumulation relax to zero and obtain a torque value independent of this parameter. Finally, we investigated the influence of the usually neglected [9] spin dephasing length λ_φ on the computation of the torque. Fig. 6 shows, that for values of λ_φ less than 3 nm, its contribution to the torque is substantial and cannot be neglected for accurately describing the magnetization dynamics.

V. Conclusion

In this work we presented a method of applying the spin drift-diffusion approach for computing the torques acting on the magnetization in an MTJ structure. The current is successfully described by modeling the tunnel barrier as a poor conductor, with an electrical conductivity locally depending on the relative magnetization orientation in the ferromagnetic layers. The spin accumulation is preserved through the middle layer, as is the case in an ideal barrier, by taking an infinite spin-flip length and a diffusion coefficient much larger than the one in the ferromagnetic layers. We showed that the contacts must be chosen long enough to not influence the torque values, and that the spin dephasing length contribution becomes significant only, if the corresponding length is below 3 nm. The generalized spin and charge drift-diffusion approach can be successfully applied to determine the torques acting in an STT-MRAM cell.

Acknowledgment

This work was supported by the *Austrian Federal Ministry for Digital and Economic Affairs* and the *National Foundation for Research, Technology and Development*.

References

[1] S. Aggarwal, H. Almasi, M. DeHerrera, B. Hughes, S. Ikegawa *et al.*, "Demonstration of a Reliable 1 Gb Standalone Spin-Transfer Torque MRAM for Industrial Applications," *Proceedings of the IEDM*, pp. 2.1.1–2.1.4, 2019.

[2] K. Lee, J. H. Bak, Y. J. Kim, C. K. Kim, A. Antonyan *et al.*, "1Gbit High Density Embedded STT-MRAM in 28nm FDSOI Technology," *Proceedings of the IEDM*, pp. 2.2.1–2.2.4, 2019.

[3] V. B. Naik, K. Lee, K. Yamane, R. Chao, J. Kwon *et al.*, "Manufacturable 22nm FD-SOI Embedded MRAM Technology for Industrial-Grade MCU and IOT Applications," *Proceedings of the IEDM*, pp. 2.3.1–2.3.4, 2019.

[4] G. Hu, J. J. Nowak, M. G. Gottwald, S. L. Brown, B. Doris *et al.*, "Spin-Transfer Torque MRAM with Reliable 2 ns Writing for Last Level Cache Applications," *Proceedings of the IEDM*, pp. 2.6.1–2.6.4, 2019.

[5] W. J. Gallagher, E. Chien, T. W. Chiang, J. C. Huang, M. C. Shih *et al.*, "22nm STT-MRAM for Reflow and Automotive Uses with High Yield, Reliability, and Magnetic Immunity and with Performance and Shielding Options," *Proceedings of the IEDM*, pp. 2.7.1–2.7.4, 2019.

[6] S. Sakhare, M. Perumkunnil, T. H. Bao, S. Rao, W. Kim *et al.*, "Enablement of STT-MRAM as Last Level Cache for the High Performance Computing Domain at the 5nm Node," *Proceedings of the IEDM*, pp. 18.3.1-18.3.4, 2018.

[7] J. G. Alzate, U. Arslan, P. Bai, J. Brockman, Y. J. Chen *et al.*, "2 MB Array-Level Demonstration of STT-MRAM Process and Performance Towards L4 Cache Applications," *Proceedings of the IEDM*, pp. 2.4.1–2.4.4, 2019.

[8] J. C. Slonczewski, "Currents, Torques, and Polarization Factors in Magnetic Tunnel Junctions," *Physical Review B,* vol. 71, p. 024411, 2004.

[9] C. Abert *et al.*, "A Three-Dimensional Spin-Diffusion Model for Micromagnetics," *Scientific Reports*, vol. 5, p. 14855, 2015.

[10] S. Lepadatu, "Unified Treatment of Spin Torques using a Coupled Magnetisation Dynamics and Three-Dimensional Spin Current Solver," *Scientific Reports*, vol. 7, p. 12937, 2017.

[11] W. Skowronski, M. Czapkiewicz, S. Zietek, J. Checinski, M. Frankowski *et al.*, "Understanding Stability Diagram of Perpendicular Magnetic Tunnel Junctions," *Scientific Reports*, vol. 7, p. 10172, 2017.

[12] S.Fiorentini, R. L. de Orio, W. Goes, J. Ender and V. Sverdlov, "Comprehensive Comparison of Switching Models for Perpendicular Spin-Transfer Torque MRAM Cells," *Proceedings of the SISPAD*, pp. 57–60, 2019.